

Red phosphorescence in Sr₄Al₁₄O₂₅: Cr³⁺, Eu²⁺, Dy³⁺ through persistent energy transfer

Ruixia Zhong, Jiahua Zhang, Xia Zhang, Shaozhe Lu, and Xiao-jun Wang

Citation: *Appl. Phys. Lett.* **88**, 201916 (2006); doi: 10.1063/1.2205167

View online: <http://dx.doi.org/10.1063/1.2205167>

View Table of Contents: <http://apl.aip.org/resource/1/APPLAB/v88/i20>

Published by the [American Institute of Physics](#).

Additional information on *Appl. Phys. Lett.*

Journal Homepage: <http://apl.aip.org/>

Journal Information: http://apl.aip.org/about/about_the_journal

Top downloads: http://apl.aip.org/features/most_downloaded

Information for Authors: <http://apl.aip.org/authors>

ADVERTISEMENT



HAVE YOU HEARD?

Employers hiring scientists
and engineers trust
physicstoday JOBS



<http://careers.physicstoday.org/post.cfm>

Red phosphorescence in $\text{Sr}_4\text{Al}_{14}\text{O}_{25}$: Cr^{3+} , Eu^{2+} , Dy^{3+} through persistent energy transfer

Ruixia Zhong, Jiahua Zhang,^{a),b)} Xia Zhang, and Shaozhe Lu

Key Laboratory of Excited State Processes, Changchun Institute of Optics, Fine Mechanics and Physics, Chinese Academy of Sciences, Changchun 130033, China and Graduate School of Chinese Academy of Sciences, Beijing 100039, China

Xiao-jun Wang^{a)}

Key Laboratory of Excited State Processes, CIOMP, CAS, Changchun 130033, China and Department of Physics, Georgia Southern University, Statesboro, Georgia 30460

(Received 17 January 2006; accepted 4 April 2006; published online 17 May 2006)

Cr^{3+} , Eu^{2+} , and Dy^{3+} codoped $\text{Sr}_4\text{Al}_{14}\text{O}_{25}$ has been synthesized by solid-state reaction. Long persistent phosphorescence in red of Cr^{3+} and in blue of Eu^{2+} has been observed in this system with persistence times of over 2 h for the red and 10 h for the blue. Red phosphorescence is performed through persistent energy transfer from Eu^{2+} to Cr^{3+} , converting the blue to the red. Concentration effect is analyzed based on energy transfer. The calculated results are in good agreement with the experimental data. The different decay patterns of the red and blue phosphorescence are measured and discussed. © 2006 American Institute of Physics. [DOI: 10.1063/1.2205167]

Long persistent phosphorescent materials have long been of interest for various displays and signing applications.¹⁻⁴ At the present, several oxide long-persistent phosphors exhibiting high brightness of blue and green phosphorescence and better chemical stability over sulfides are commercially available.^{1,2} However, the oxide phosphors with long persistent red phosphorescence have not been obtained yet, thus still commercially limited to sulfides, MS: Eu ($M=\text{Ca}, \text{Sr}$).⁵

To obtain persistent phosphorescence in various colors, the idea of persistent energy transfer is proposed,⁶ by which green, orange, and red phosphorescence are observed.^{4,7,8} As it is known, strontium aluminates doped with Eu^{2+} possess high quantum efficiency, long persistence of the phosphorescence, and good stability, indicating their good practical prospects.^{1,2} In particular, $\text{Sr}_4\text{Al}_{14}\text{O}_{25}$: Eu^{2+} , Dy^{3+} has demonstrated excellent blue (490 nm) phosphorescence,⁹ while Cr^{3+} , as an activator with red emission, has been widely used in luminescent materials, such as (yttrium aluminum garnet) YAG: Cr^{3+} .¹⁰ If Cr^{3+} can be incorporated into $\text{Sr}_4\text{Al}_{14}\text{O}_{25}$: Eu^{2+} , Dy^{3+} lattices, and energy transfer between Eu^{2+} and Cr^{3+} are efficient, then Cr^{3+} activated red phosphorescence may be expected.

This letter reports the synthesis and phosphorescence properties of $\text{Sr}_4\text{Al}_{14}\text{O}_{25}$: Cr^{3+} , Eu^{2+} , Dy^{3+} phosphors. In this system, the persistent red phosphorescence at 693 nm of Cr^{3+} is obtained through persistent energy transfer from the Eu^{2+} to Cr^{3+} , leading to conversion of persistent blue phosphorescence into the red one. The Cr^{3+} concentration dependent intensity ratio of the red emission of Cr^{3+} to the blue of Eu^{2+} is analyzed based on energy transfer. The calculated results are in good agreement with the experimental data. The different decay patterns of the red and blue phosphorescence are measured and discussed.

Samples of $\text{Sr}_4\text{Al}_{14}\text{O}_{25}$: Eu^{2+} , Dy^{3+} , Cr^{3+} have been synthesized by high temperature solid state reaction. The starting materials are SrCO_3 , Al_2O_3 , Eu_2O_3 (99.9%), Dy_2O_3

(99.9%), Cr_2O_3 and H_3BO_3 . The powder samples have been weighed according to $4\text{SrO}+7\text{Al}_2\text{O}_3+0.4\text{B}_2\text{O}_3$, with different concentrations of Eu, Cr, and 2 at % Dy. All the mixtures are grounded for 1 h, then preheated at 1000 °C in air for 4 h, and finally sintered at 1350 °C in a reducing atmosphere for 7 h. Emission and excitation spectra are measured with a Hitachi F-4500 Spectra-fluorometer. In fluorescence lifetime measurements, the third (355 nm) harmonic of a Nd-YAG laser (Spectra-Physics, GCR 130) is used as an excitation source, and the signal is detected with a Tektronix digital oscilloscope model (TDS 3052). The crystalline structure of the sample is investigated by x-ray diffraction (XRD) using a Siemens D-500 equipment with a Cu target radiation source. XRD pattern of Cr^{3+} , Eu^{2+} , and Dy^{3+} doped samples presents a pure $\text{Sr}_4\text{Al}_{14}\text{O}_{25}$ phase belonging to the orthorhombic system with space group of P_{mna} . $\text{Sr}_4\text{Al}_{14}\text{O}_{25}$ is composed of octahedral AlO_6 anion and tetrahedral AlO_4 groups.¹¹

Figure 1 depicts the emission and excitation spectra of $\text{Sr}_4\text{Al}_{14}\text{O}_{25}$: 1% Eu^{2+} and 2% Dy^{3+} (dash lines) and that of $\text{Sr}_4\text{Al}_{14}\text{O}_{25}$: 1% Cr^{3+} , $x\%$ Eu^{2+} , and 2% Dy^{3+} ($x=0, 0.1, 0.5, 1, 2, \text{ and } 3$; solid lines). In $\text{Sr}_4\text{Al}_{14}\text{O}_{25}$: 1% Eu^{2+} and 2% Dy^{3+} , the emission and excitation bands correspond to the $f-d$ transition of Eu^{2+} . The emission spectrum consists of a strong band at 490 nm with a weak band at 400 nm, which are attributed to different Eu^{2+} centers in $\text{Sr}_4\text{Al}_{14}\text{O}_{25}$.⁹ In $\text{Sr}_4\text{Al}_{14}\text{O}_{25}$: 1% Cr^{3+} , $x\%$ Eu^{2+} , and 2% Dy^{3+} , the ${}^2E-{}^4A_2$ emissions of Cr^{3+} at 693 nm are observed under 330 nm excitation. The excitation spectra of the 693 nm emissions consist of the ${}^4A_2-{}^4T_1(F)$ absorption at 420 nm and ${}^4A_2-{}^4T_2(F)$ absorption at 570 nm of Cr^{3+} , and the $f-d$ absorption of Eu^{2+} in ultraviolet region. The intensities of the 570 nm excitation bands are normalized. From Fig. 1, the 490 nm emission band of Eu^{2+} has spectral overlaps with the absorption bands of Cr^{3+} , indicating the possibility of energy transfer from Eu^{2+} to Cr^{3+} . It can also be seen that the excitation bands originating from $f-d$ transition of Eu^{2+} in ultraviolet region grow up with the increase of Eu^{2+} concentrations when only the red emission at 693 nm of Cr^{3+} is monitored. Furthermore, the red emission of Cr^{3+} increases with the increase of

^{a)} Authors to whom correspondence should be addressed.

^{b)} Electronic mail: zjiahua@public.cc.ji.cn

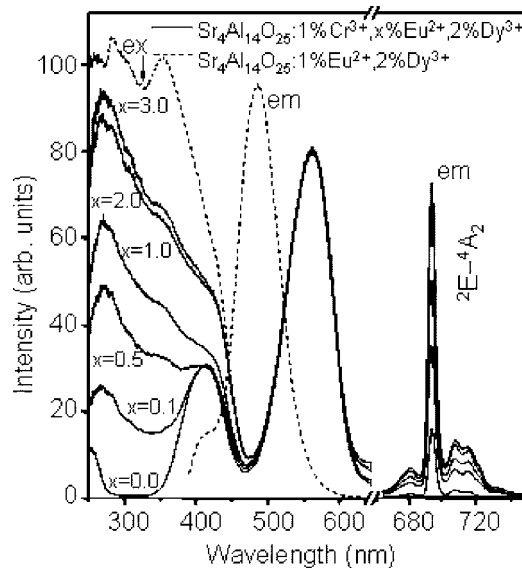


FIG. 1. Emission ($\lambda_{\text{ex}}=330$ nm) and excitation spectra of $\text{Sr}_4\text{Al}_{14}\text{O}_{25}:x\% \text{Cr}^{3+}, 1\% \text{Eu}^{2+}, 2\% \text{Dy}^{3+}$ (solid lines, $x=0, 0.1, 0.5, 1, 2,$ and 3 ; $\lambda_{\text{em}}=693$ nm), and $\text{Sr}_4\text{Al}_{14}\text{O}_{25}:1\% \text{Eu}^{2+}, 2\% \text{Dy}^{3+}$ (dashed lines, $\lambda_{\text{em}}=490$ nm).

Eu^{2+} concentrations under 330 nm excitation, by which only Eu^{2+} can be excited because there is no absorption of Cr^{3+} at this wavelength, as shown in Fig. 1. These results strongly indicate the performance of energy transfer from Eu^{2+} to Cr^{3+} in $\text{Sr}_4\text{Al}_{14}\text{O}_{25}: \text{Cr}^{3+}, \text{Eu}^{2+}, \text{Dy}^{3+}$.

Figure 2 shows the emission spectra of $\text{Sr}_4\text{Al}_{14}\text{O}_{25}: x\% \text{Cr}^{3+}, 1\% \text{Eu}^{2+},$ and $2\% \text{Dy}^{3+}$ ($x=0, 0.5, 1, 2, 3, 4,$ and 5) under 330 nm excitation, where the intensities of the blue bands at 490 nm are normalized. When maintaining the Eu^{2+} concentration and increasing the Cr^{3+} contents up to 4%, the red lines at 693 nm from Cr^{3+} are enhanced, indicating the increase of energy transfer efficiency since Cr^{3+} cannot be

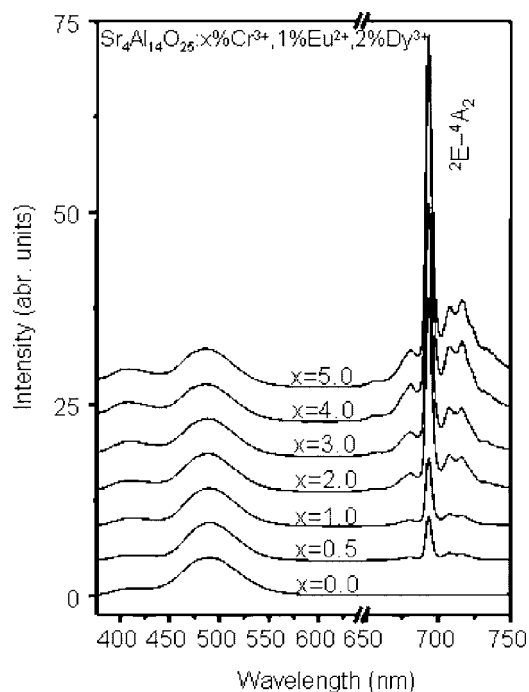


FIG. 2. Emission spectra of $\text{Sr}_4\text{Al}_{14}\text{O}_{25}:x\% \text{Cr}^{3+}, 1\% \text{Eu}^{2+},$ and $2\% \text{Dy}^{3+}$ ($x=0, 0.5, 1, 2, 3, 4,$ and 5) under 330 nm excitation. The intensities of the blue bands at 490 nm are normalized.

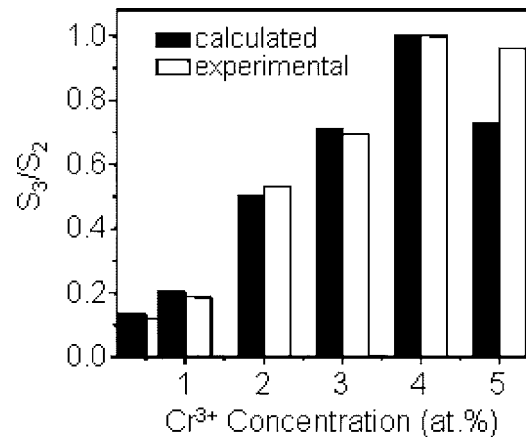


FIG. 3. Calculated and experimental ratios (S_3/S_2) of the red emission to the blue at 490 nm for different Cr^{3+} concentrations. The ratios are scaled to the maximum.

excited by 330 nm directly. The addition of Cr^{3+} ions leads to an increase of Cr^{3+} surrounding the Eu^{2+} ion, thus resulting in more efficient energy transfer. When the concentration of Cr^{3+} is higher than 4%, the intensity of the red lines begins to decrease. This is attributed to concentration quenching of Cr^{3+} ions.

In order to analyze the change in the intensity ratio of the red to blue emissions with Cr^{3+} concentrations, the lifetimes of 400 (τ_1), 490 (τ_2), and 693 nm (τ_3) emissions in $\text{Sr}_4\text{Al}_{14}\text{O}_{25}: x\% \text{Cr}^{3+}, 1\% \text{Eu}^{2+}, 2\% \text{Dy}^{3+}$ ($x=0, 0.5, 1, 2, 3, 4,$ and 5) are measured. All the decays can be described as a single exponential function. The energy transfer processes can be described as follows: the three emitting centers at 400, 490, and 693 nm are labeled by 1, 2, and 3, respectively, and the energy transfer from their center is considered. In static excitation, the rate equation for center 3 is written as

$$W_{13}n_1 + W_{23}n_2 = n_3/\tau_3, \quad (1)$$

where n_i and W_{i3} are population of center i and energy transfer rate from center i to center 3, respectively. If the emission intensity and radiative transition rate of center i are denoted by S_i and γ_i , respectively, using Eq. (1) the intensity ratio of the red emission of Cr^{3+} to the blue one at 490 nm of Eu^{2+} is determined by the following equation:

$$\frac{S_3}{S_2} = \frac{\gamma_3 \tau_3 W_{23}}{\gamma_2} \left(1 + \frac{\gamma_2 W_{13} S_1}{\gamma_1 W_{23} S_2} \right), \quad (2)$$

where $W_{13} = 1/\tau_1 - 1/\tau_1(0)$, $W_{23} = 1/\tau_2 - 1/\tau_2(0)$, and $\tau_i(0)$ is the fluorescence lifetime of center i when Cr^{3+} concentration is zero. The S_1/S_2 integral intensity ratio of the 400 nm emission to the 490 nm emission can be calculated according to the emission spectra in Fig. 2. The γ_1 and γ_2 are obtained from intrinsic lifetime measurements of 400 and 490 nm emissions, respectively, in $\text{Sr}_4\text{Al}_{14}\text{O}_{25}: 0.1\% \text{Eu}^{2+}$ to avoid concentration and nonradiative transition effects. Similarly, γ_3 is obtained in $\text{Sr}_4\text{Al}_{14}\text{O}_{25}: 0.1\% \text{Cr}^{3+}$. Using Eq. (2) and the measured lifetimes, the S_3/S_2 intensity ratios at various Cr^{3+} concentrations are calculated and scaled to the maximum, as presented in Fig. 3. For comparison, the intensity ratios obtained directly from the emission spectra are also given in Fig. 3. It can be seen that the calculated data are in good agreement with the experimental ones.

Owing to energy transfer, Cr^{3+} activated persistent red phosphorescence has been observed besides the Eu^{2+} acti-

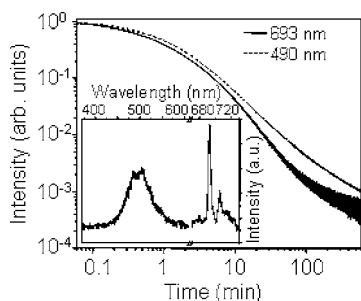


FIG. 4. Time decay curves of the phosphorescence at 490 and 693 nm of $\text{Sr}_4\text{Al}_{14}\text{O}_{25}$: 1% Cr^{3+} , 0.5% Eu^{2+} , 2% Dy^{3+} after irradiation with xenon lamp for 5 min. The phosphorescence spectrum is presented in the inset.

vated blue phosphorescence in $\text{Sr}_4\text{Al}_{14}\text{O}_{25}$: Cr^{3+} , Eu^{2+} , Dy^{3+} . The phosphorescence spectra measured at 10 min after removal of exposure source are shown in Fig. 4 (insert). The phosphorescence spectra are the same as the fluorescence spectra in Fig. 2. Figure 4 presents the time decay curves of the blue phosphorescence at 490 nm and the red at 693 nm in $\text{Sr}_4\text{Al}_{14}\text{O}_{25}$: 1% Cr^{3+} , 0.5% Eu^{2+} , 2% Dy^{3+} after irradiation with xenon lamp for 5 min. It can be seen that the initial decay rate of the red is similar to the blue but gradually the red begins to decay faster, and finally both of them become the same rate again. In the system of $\text{Sr}_4\text{Al}_{14}\text{O}_{25}$: Cr^{3+} , Eu^{2+} , Dy^{3+} , Dy^{3+} may act as trap centers, capturing the free holes similar in other strontium aluminate systems.^{1,12,13} Because the Cr^{3+} replaces Al^{3+} , there exist two types of Dy^{3+} , one surrounded mainly by Al called Dy1, and the other by at least one near-neighbor Cr called Dy2. It is speculated that the former trap may be deeper than the latter. In other words, the incorporation of Cr^{3+} ions results in shallow nearby hole traps. For simplicity, the energy transfer process from Eu^{2+} to Cr^{3+} ions may be considered as two parts, the first part being the short-range energy transfer between the Eu^{2+} and Cr^{3+} ions. In this case, Eu^{2+} is surrounded by both Dy1 and Dy2 at a short distance, leading both Dy1 and Dy2 to contribute to phosphorescence. The second part is named long-range energy transfer between the two ions. In this case, Eu^{2+} is surrounded by Dy1 at a short distance, leading only Dy1 to contribute to the phosphorescence. Due to the efficient energy transfer in short distance, the red afterglow is mainly generated by those Cr^{3+} ions close to Eu^{2+} ions and negligibly by those far from it. Therefore, the main component of the red phosphorescence decays with the larger rates as determined by the incorporation of Dy1 and shadow trap Dy2. A small part of it decays slower by the deeper trap Dy1 only. In contrary, the blue emissions prefer an inefficient energy transfer, leading the main part of the blue phosphorescence to decay slower and a small part to decay faster. This results in a faster decay of both the blue and red phosphorescence at the beginning. The decay of the blue phosphores-

cence becomes slower much earlier than the red because the main components of blue are slow. In this time, the red certainly exhibits faster decay than the blue. As the faster components of the red one are exhausted after a sufficient time, the slower components of the red begins to play an important role, presenting slow decay as the blue does. As a whole, faster decay of the red afterglow is interpreted as the role of the shallow traps induced by Cr^{3+} ions.

In conclusion, long lasting red phosphorescence is observed in $\text{Sr}_4\text{Al}_{14}\text{O}_{25}$: Cr^{3+} , Eu^{2+} , Dy^{3+} through persistence energy transfer from Eu^{2+} to Cr^{3+} . The energy transfer leads to the following results: (1) the intensity of the red emission of Cr^{3+} at 693 nm is enhanced by increasing the concentrations of optically excited Eu^{2+} ; (2) as the concentration of Eu^{2+} and Dy^{3+} are fixed, the ratio of the red emission of Cr^{3+} to the blue of Eu^{2+} increases with increasing Cr^{3+} concentrations when only Eu^{2+} is optically excited; (3) the ratio of the red emission (693 nm) to the blue (490 nm) by experiment is consistent with the theoretical calculation basing on energy transfer and lifetime measurements; (4) the fluorescence and phosphorescence spectra are identical both for the red and blue bands. The red phosphorescence decays faster than the blue while the persistent time is over 2 h for the red afterglow and more than 10 h for the blue. The relatively fast decay of the red afterglow to that of the blue is interpreted as the contribution of the more shallow traps induced by Cr^{3+} .

This work is financially supported by the ‘‘One Hundred Talents Project’’ from the Chinese Academy of Sciences, the MOST of China (Grant No. 2006CB601104), and by the National Natural Science Foundation of China (Grant No. 10574128).

¹T. Matsuzawa, Y. Aoki, N. Takeuchi, and Y. Murayama, *J. Electrochem. Soc.* **143**, 2670 (1996).

²W. Jia, H. Yuan, L. Lu, H. Liu, and W. M. Yen, *J. Cryst. Growth* **200**, 179 (1999).

³N. Kodama, T. Takahashi, M. Yamaga, Y. Tani, J. Qiu, and K. Hirao, *Appl. Phys. Lett.* **75**, 1715 (1999).

⁴D. Jia, R. S. Meltzer, W. M. Yen, W. Jia, and X. J. Wang, *Appl. Phys. Lett.* **80**, 1535 (2002).

⁵D. Jia, B. Wu, and J. Zhu, Canadian Patent No. 00,100,388 (2000).

⁶W. M. Yen, D. Jia, W. Jia, and X. J. Wang, U.S. Patent No. 6,952,536 (2005).

⁷D. Jia, X. J. Wang, W. Jia, and W. M. Yen, *J. Appl. Phys.* **93**, 148 (2003).

⁸X. J. Wang, D. Jia, and W. M. Yen, *J. Lumin.* **102–103**, 34 (2003).

⁹Y. H. Lin, Z. L. Tang, Z. T. Zhang, and C. W. Nan, *Appl. Phys. Lett.* **81**, 996 (2002).

¹⁰I. Matsubara, M. Paranthaman, S. W. Allison, M. R. Cates, D. L. Beshears, and D. E. Holcomb, *Mater. Res. Bull.* **35**, 217 (2000).

¹¹D. Wang and M. Q. Wang, *J. Mater. Sci.* **34**, 4959 (1999).

¹²H. Aizawa, S. Komuro, T. Katsumata, S. Sato, and T. Morikawa, *Thin Solid Films* **496**, 179 (2006).

¹³Z. X. Yuan, C. K. Chang, D. L. Mao, and W. J. Ying, *J. Alloys Compd.* **377**, 268 (2004).